A Meta Distribution-based Fine-Grained Analysis for Contention-based WiFi Backscatter Networks

Yulei Wang[1], Qinglin Zhao[1], Li Feng[1], MengChu Zhou[2], Meng Shen[3], Yu Luo[4], and Yi Sun[5]
[1] *School of Computer Science and Engineering, Macau University of Science and Technology, Macau 999078, China*
[2] *Department of Electrical and Computer Engineering, New Jersey Institute of Technology, Newark, NJ 07102, USA*
[3] *School of Cyberspace Science and Technology, Beijing Institute of Technology, Beijing 100081, China*
[4] *School of Computer Science, Guangdong University of Technology, Guangzhou 510006, China*
[5] *Institute of Computing Technology, Chinese Academy of Sciences, Beijing 100045, China*
E-mail: wylpaper@126.com, {qlzhao, lfeng}@must.edu.mo, zhou@njit.edu,
shenmeng@bit.edu.cn, yuluo@gdut.edu.cn, sunyi@ict.ac.cn

***Abstract*—WiFi backscatter communication has gained many applications, but its performance characteristics remains to be analyzed. Yet they are crucial for its practical deployment. While existing research has investigated the success probability of backscatter tags in contention-based WiFi backscatter networks (CWBNs), it has focused solely on the first-order statistic of the signal-to-interference-plus-noise ratio (SINR). In this paper, we present a meta distribution-based fine-grained analysis that provides high-order statistics of SINR and characterizes the disparity among backscatter transmission links in CWBNs. Leveraging stochastic geometry, we derive mathematical expressions for the b-th moments of conditional success probability and its meta distribution. The extensive Monte-Carlo simulation results validate the accuracy of our proposed theoretical model and demonstrate its outstanding value to help us understand the overall performance of CWBNs.**

***Index Terms*—Meta distribution, stochastic geometry, WiFi backscatter networks**

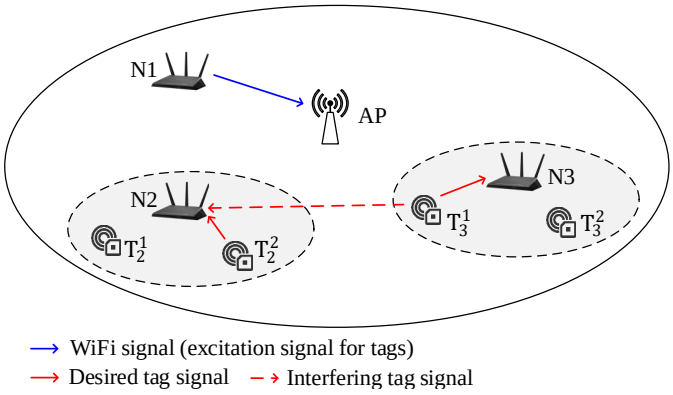

Fig. 1. An overview of CWBN.

I. Introduction

WiFi backscatter applications (i.e., environmental monitoring, wearable devices) have been widely employed in both outdoor and indoor settings. Leveraging their low-cost and energy-efficient advantages, these applications provide significant convenience to our lives while also imposing substantial data transmission requirements. To further explore the full potential of WiFi backscatter communication, contention-based WiFi backscatter networks (CWBNs) have been developed [1]. In CWBNs, backscatter tags contend to transmit their data to nearby WiFi nodes by reflecting the transmitting ambient WiFi signals, then nodes relay the collected tag data to a remote access point (AP). As a result, CWBNs significantly extend tags' transmission range and improve backscatter throughput.

Understanding the performance characteristics of WiFi backscatter networks is crutial for their practical deployment. Prior studies (i.e., [1]–[3]) have theoretically evaluated the transmission performance of backscatter networks. However, these analyses often overlook critical spatial factors, such as the location distribution of tags, leading to limited insights. To address this challenge, researchers have turned to stochastic geometry (SG) approach [4]–[6] to investigate the impact of tags' location randomness on network performance. Unfortunately, existing analyses typically provide only the first-order statistic of the signal-to-interference-plus-noise ratio (SINR), such as standard success (coverage) probability. This metric represents the mean conditional success probability (CSP) given a specific spatial realization of tags. While informative for average network performance, it fails to capture the disparity among backscatter transmission links. Consider the following example with two networks A and B: in Network A, 50% of the users has a CSP of 0 while the other 50% have a CSP of 1; in contrast, Network B exhibits a uniform CSP of 0.5 for all users. Despite both networks having the same standard success probability of 0.5, they exhibit significant differences. This discrepancy naturally raises the question: *what fraction of users achieve a desired link reliability x for a given SINR threshold in the backscatter networks*? To address this, meta distribution (MD), the complementary cumulative distribution function (CCDF) of the CSP, was recently proposed in [7]–[9] and further explored in various fields (i.e., [10]–[14]). Reconsider the above example with the given reliability x: if $x = 0.4$, 50% of users achieve the reliability in Network A, while all users achieve it in Network B; if $x = 0.6$, 50% of

This work is funded in part by the Science and Technology Development Fund, Macau SAR (Grant Nos. 0093/2022/A2, 0076/2022/A2 and 0008/2022/AGJ), in part by Guangzhou Nansha Science and Technology Planning Project (File No. 2023ZD002). Q. Zhao is the corresponding author.

users achieve the reliability in Network A, while none achieve it in Network B. This disparity, uncovered by MD, highlights crucial differences in wireless networks.

A. Motivation

The current state-of-the-art, which adopts an SG approach, primarily focuses on analyzing the standard success probability of tags in backscatter networks. However, it lacks an accurate analytical model to evaluate the reliability of backscatter transmission links in CWBNs. In fact, this problem is not easy, since it is influenced by the two critical factors:

- Location randomness: In CWBNs, nodes and tags are randomly deployed in practical environments.
- Contention randomness: In CWBNs, tags contend to transmit their data to nodes by reflecting the transmitting ambient WiFi signals.

This motivates us to develop an MD-based theoretical model to provide more fine-grained analysis and capture the disparity among individual backscatter transmission links in CWBNs.

B. Our Contributions

To the best of our knowledge, this paper is the first to leverage MD for evaluating the reliability of backscatter transmission links in CWBNs. Specifically, we summarize our contributions as follows:

- We capture the random locations of nodes and tags using an SG approach and characterize the random contention of tags using probability theory.
- We derive mathematical expressions for the b-th moments of CSP and its MD, which incorporate various network parameters (i.e., the density of nodes and tags, the SINR threshold, the transmission reliability x).
- We conduct extensive Monte-Carlo simulations, which validates the accuracy of our theoretical model.

This study provides novel insights that enhance our understanding of the performance disparity among individual backscatter transmission links and is helpful to configure suitable parameters for reliable CWBNs.

The remainder of the paper is organized as follows. Section II reviews the related work. Section III outlines the system model. Section IV presents the meta distribution analysis. Section V verifies the accuracy of our theoretical model. Section VI concludes this paper.

II. Related Work

Backscatter networks, in which tags exploit surrounding excitation signals (e.g., cellular and WiFi signals) to convey data, have recently drawn great attention [1]–[6], [15]–[17]. This section provides a literature review on the performance analysis of backscatter networks using traditional and SG approaches.

A. Performance Analysis with Traditional Approach

Many studies analyze the performance of backscatter networks using traditional approach, which primarily focus on the transmission randomness of tags. For example, Ma *et al.* [2] analyze the system throughput of WiFi backscatter networks, where the tags contend to convey data to an AP following binary exponential backoff algorithm. Cao *et al.* [3] construct an enhanced 3-D Markov model to analyze the throughput and energy performance of the backscatter networks, which characterizes the backscatter contention with dual-backoff mechanism and takes into account the tags' channel sensing errors. Wang *et al.* [1] theoretically analyze the transmission throughput of nodes and tags in proposed CWBNs, which captures the transmission randomness of nodes and tags. All these performance analyses focus solely on the transmission randomness of tags, while overlook critical spatial factors, such as the location distribution of tags, resulting in limited insights.

B. Performance Analysis with SG Approach

Researchers have turned to SG approach, which delves into the study of random spatial patterns, to gain deeper insights into the impacts of tags' location randomness on the performance of backscatter networks. According to the performance metrics, these studies can be classified into two categories: success probability-based and MD-based analysis.

1) Success Probability-based Analysis: Most studies have adopted SG approach to model the location distribution of tags and analyzed the success probability of backscatter transmission links. For instance, Shi *et al.* [4] theoretically analyze the active and successful probabilities of backscatter transmitters in ambient backscatter underlying cellular networks, where the location distribution of backscatter transmitters is modelled by a homogeneous Poisson point process (HPPP). Wang *et al.* [5] explore the coverage probability and spatial throughput of tags in multi-cluster backscatter networks using SG approach, which captures the location randomness of emitters, tags, and the inter-cluster and intra-cluster interferences. The short paper [6] just analyze the success probability of tags-to-WiFi transmissions in CWBNs, which models the location distributions of nodes and tags with two HPPPs. While these studies provide some new insights into the average network performance, but they fail to capture the individual backscatter transmission link behaviors and evaluate their reliability in CWBNs.

2) Meta Distribution-based Analysis: MD provides a more precise characterization of a typical transmission link compared to the standard success probability. Despite its potential, no existing work has applied MD to investigate the reliability of backscatter transmissions in backscatter networks. In light of the location randomness and contention randomness inherent in CWBNs, this paper takes a pioneering step by developing an MD-based theoretical model. This model provides a fine-grained analysis, capturing the disparity among individual backscatter transmission links within CWBNs.

III. System Model

This section presents the system model in terms of the network deployment, the interference and channel model.

A. Network Deployment

We consider a typical CWBN which consists of one AP, mutliple nodes and numerous tags, as shown in Fig. 1. In this network, the coverage of AP forms a circular cell $A \subset \mathbb{R}^2$ with radius d, the coverage of each node forms a circular subcell B with radius $\widetilde{d}$. The nodes and tags are randomly located in the cell. We model the locations of the nodes and tags by two independent homogeneous Poisson point processes (HPPPs) $\Phi_w \subset \mathbb{R}^2$ and $\Phi_b \subset \mathbb{R}^2$ with densities λ_w and λ_b ($\lambda_b \gg \lambda_w$), respectively. Besides, we assume that the subcells are disjoint in the plane.

B. Interference Model

As Fig. 1 shows, when a node (i.e., N1) is transmitting a WiFi signal to the AP, the tags in subcells of other nodes (except N1) can exploit this ambient WiFi signal to perform backscatter contention and transmission. For more details, please refer to [1].

We take an example to present the interference model. When N2 receives the desired tag signal from tag T_2^2 which wins the backscatter contention within the subcell of N2, it also suffers from the interfering tag signals due to the concurrent backscatter transmissions (e.g., T_3^1-to-N3 transmission) in the subcells of other nodes (except N1 and N2). We assume that there is only one tag that wins the contention in each subcell. Hence, the density of interfering tags λ_b' is given by $\lambda_b' = \lambda_w - 2/|A|$, where $|A| = \pi d^2$ is the area of AP cell [6].

C. Channel Model

We assume that backscatter signals undergo both large- and small-scale fading effects. The former is characterized by the power-law path loss model $R^{-\alpha}$, where R is the distance between the transmitter and the receiver, α is the path loss exponent with usually $2 < \alpha < 6$ [5], [18]; the latter is characterized by the Rayleigh fading model with power fading coefficient H (square of the amplitude fading coefficient) [19], [20], which follows exponential distribution with unit mean, i.e., $H \sim exp(1)$. We also assume that the thermal noise at the receiver is additive white Gaussian noise with zero mean and variance σ^2.

With above channel model, we can express the signal-to-interference-plus-noise ratio (SINR) measured at the node as

$$SINR = \frac{P_r}{I + \sigma^2} \tag{1}$$

In (1), $P_r = P_0 H_0 R_0^{-\alpha}$ and $I = \sum_{i \in \Phi_b'} P_0 H_i R_i^{-\alpha}$ denote the received power of desired tag signal and interfering tag signals at the node, respectively. Wherein, P_0 is the reflection power of each tag, $\Phi_b' \subset \Phi_b$ is the set of interfering tags with density λ_b', H_0 and R_0 denote the channel power gain and distance between the tag and its node, respectively, H_i and R_i denote the channel power gain and distance between the interfering tag i and the receiving node, respectively.

IV. Meta Distribution-based Theoretical Model

This section presents a meta distribution (MD)-based theoretical model to provide fine-grained analysis for CWBNs.

Recall that a tag contends to transmit its data to its node by exploiting ambient WiFi signals in a CWBN. As Fig. 1 shows, tag T_2^2 contends to transmit its data to N2 by exploiting the N1-to-AP WiFi signal. Hence, a successful backscatter transmission should satisfy the following two conditions:

1) Only one tag wins the backscatter contention in its subcell and transmits data to its node. This event is denoted as $\Psi = 1$;
2) The tag's data is successfully received by its node, that is, the SINR measured at this node exceeds a certain threshold θ. This event is denoted as $SINR > \theta$.

Let $\mathbb{P}_b^s(\theta)$ denote the conditional success probability (CSP) of a backscatter transmission link (e.g., T_2^2-to-N2) for a given SINR threshold θ conditioned on a point process of tags Φ_b. Thus, $\mathbb{P}_b^s(\theta)$ is defined as

$$\begin{aligned} \mathbb{P}_b^s(\theta) &\triangleq \mathbb{P}(\Psi = 1, SINR > \theta | \Phi_b) \\ &= \mathbb{P}(\Psi = 1 | \Phi_b) \cdot \mathbb{P}(SINR > \theta | \Psi = 1, \Phi_b) \end{aligned} \tag{2}$$

The MD quantifies the probability of $\mathbb{P}_b^s(\theta) > x, x \in [0,1]$. It reflects the reliability of a link and hence provides more fine-grained information on network performances. Let $\bar{F}_{\mathbb{P}_b^s(\theta)}(x)$ denote the MD of a backscatter transmission link, which is formulated as the complementary cumulative distribution function (CCDF) of CSP $\mathbb{P}_b^s(\theta)$ [7], i.e.,

$$\bar{F}_{\mathbb{P}_b^s(\theta)}(x) \triangleq \mathbb{P}(\mathbb{P}_b^s(\theta) > x), x \in [0,1] \tag{3}$$

To calculate $\bar{F}_{\mathbb{P}_b^s(\theta)}(x)$, one may resort to the Gil-Pelaez inversion theorem [7], i.e.,

$$\bar{F}_{\mathbb{P}_b^s(\theta)}(x) = \frac{1}{2} + \frac{1}{\pi} \int_0^\infty \frac{\Im\left[e^{-it\log x} M_{it}(\theta)\right]}{t} dt \tag{4}$$

where $M_b(\theta)$ (abbreviated as M_b for short) is the b-th moment of $\mathbb{P}_b^s(\theta)$, $i = \sqrt{-1}$ is the imaginary unit, $\Im[z]$ is the imaginary part of $z \in \mathbb{C}$. Though (4) provides an exact expression of $\bar{F}_{\mathbb{P}_b^s(\theta)}(x)$, it is hard to evaluate numerically and gain direct insights. We present an approximate calculation of MD with standard beta distribution by matching their first two moments [7], which yields

$$\bar{F}_{\mathbb{P}_b^s(\theta)}(x) \approx 1 - I_x\left(\frac{M_1^2 - M_1 M_2}{M_2 - M_1^2}, \frac{(M_1 - M_2)(1 - M_1)}{M_2 - M_1^2}\right) \tag{5}$$

where $I_x(\cdot,\cdot)$ is the regularized incomplete beta function [7].

The b-th moment of $\mathbb{P}_b^s(\theta)$ is obtained by taking the expectation with respect to the point process of tags Φ_b. Thus, $M_b(\theta)$ is defined as

$$M_b(\theta) \triangleq \mathbb{E}_{\Phi_b}\left[\left(\mathbb{P}_b^s(\theta)\right)^b\right] \tag{6}$$

According to (2), we can further express $M_b(\theta)$ as:

$$\begin{aligned} & M_b(\theta) \\ & = \mathbb{E}_{\Phi_b}\left[\left(\mathbb{P}(\Psi=1|\Phi_b)\cdot\mathbb{P}(SINR>\theta|\Psi=1,\Phi_b)\right)^b\right] \\ & \overset{(a)}{\approx} \mathbb{E}_{\Phi_b}\left[\mathbb{P}(\Psi=1|\Phi_b)^b\right]\cdot\mathbb{E}_{\Phi_b}\left[\mathbb{P}(SINR>\theta|\Psi=1,\Phi_b)^b\right] \\ & = \mathbb{E}_{\Phi_b}\left[\mathbb{P}(\Psi=1|\Phi_b)^b\right]\cdot M_{b|\Phi_b}(\theta) \end{aligned} \tag{7}$$

In (a), conditioned on a point process of tags Φ_b, $\mathbb{P}(\Psi=1|\Phi_b)$ is related to the contention randomness of tags in a subcell, while $\mathbb{P}(SINR>\theta|\Psi=1,\Phi_b)$ is related to the location randomness of tags. Assuming both to be independent, we can approximately obtain (a). In the following, we first express $\mathbb{E}_{\Phi_b}\left[\mathbb{P}(\Psi=1|\Phi_b)^b\right]$ and then $M_{b|\Phi_b}(\theta)$.

A. Expression of $\mathbb{E}_{\Phi_b}\left[\mathbb{P}(\Psi=1|\Phi_b)^b\right]$

Let $\Phi_b(B)$ denote the number of tags in a subcell B, which takes a value from 1 to a maximum value $\hat{m}$. Let $\mathbb{P}(\Phi_b(B)=m)$ denote the probability of m tags in a subcell B. Let $\mathbb{P}(\Psi=1|\Phi_b(B)=m)$ denote the probability that only one tag wins the channel among m tags in a subcell B. Hence, we can express $\mathbb{E}_{\Phi_b}\left[\mathbb{P}(\Psi=1|\Phi_b)^b\right]$ as

$$\begin{aligned} & \mathbb{E}_{\Phi_b}\left[\mathbb{P}(\Psi=1|\Phi_b)^b\right] \\ & = \sum_{m=1}^{\hat{m}}\mathbb{P}(\Psi=1|\Phi_b(B)=m)^b\cdot\mathbb{P}(\Phi_b(B)=m)^b \end{aligned} \tag{8}$$

Below, we calculate the two probabilities $\mathbb{P}(\Phi_b(B)=m)$ and $\mathbb{P}(\Psi=1|\Phi_b(B)=m)$ sequentially.

1) Calculation of $\mathbb{P}(\Phi_b(B)=m)$: Since the location distribution of tags follows an HPPP in a subcell, we can express $\mathbb{P}(\Phi_b(B)=m)$ as

$$\mathbb{P}(\Phi_b(B)=m) = exp(-\lambda_b|B|)\frac{(\lambda_b|B|)^m}{m!} \tag{9}$$

where $|B|=\pi\widetilde{d}^2$ is the area of each subcell B.

2) Calculation of $\mathbb{P}(\Psi=1|\Phi_b(B)=m)$: In backscatter contention, each tag in a subcell chooses a backoff counter uniformly distributed in $[0, L-1]$ for countdown. The tag that chooses the minimum backoff counter is the winner. Let l, $l=0,1,\ldots,L-1$, denote the minimum backoff counter in one contention process. Depending on whether m is equal to 1, we can express $\mathbb{P}(\Psi=1|\Phi_b(B)=m)$ as

$$\begin{aligned} & \mathbb{P}(\Psi=1|\Phi_b(B)=m) \\ & = \begin{cases} 1 & m=1 \\ \sum_{l=0}^{L-2}\binom{m}{1}\left(\frac{1}{L}\right)\left(\frac{L-1-l}{L}\right)^{m-1} & m>1 \end{cases} \end{aligned} \tag{10}$$

B. Expression of $M_{b|\Phi_b}(\theta)$

The b-th moment is obtained by taking the expectation with respect to the point process of tag Φ_b. Thus, $M_{b|\Phi_b}(\theta)$ can be expressed as

$$\begin{aligned} & M_{b|\Phi_b}(\theta) = \mathbb{E}_{\Phi_b}\left[\mathbb{P}(SINR>\theta|\Psi=1,\Phi_b)^b\right] \\ & = \mathbb{E}_{R_0,R_i}\left[\mathbb{P}\left(\frac{P_0H_0R_0^{-\alpha}}{\sum_{i\in\Phi_b'}P_0H_iR_i^{-\alpha}+\sigma^2}>\theta\middle|\Psi=1,\Phi_b\right)^b\right] \\ & = \int_0^{\widetilde{d}}\mathbb{E}_{R_i}\left[\mathbb{P}\left(\frac{P_0H_0r_0^{-\alpha}}{\sum_{i\in\Phi_b'}P_0H_iR_i^{-\alpha}+\sigma^2}>\theta\middle|\Psi=1,\Phi_b\right)^b\right] \\ & \quad\cdot f_{R_0}(r_0)\,dr_0 \\ & \overset{(a)}{=} \int_0^{\widetilde{d}}\Omega\cdot\underbrace{\mathbb{E}_{R_i}\left[\prod_{b'\in\Phi_b'}\left(\frac{1}{1+\theta r_0^{\alpha}R_i^{-\alpha}}\right)^b\right]}_{\Delta_b}\cdot f_{R_0}(r_0)\,dr_0 \end{aligned} \tag{11}$$

where $\Omega = exp\left(-b\theta\sigma^2r_0^{\alpha}/P_0\right)$, $f_{R_0}(r_0) = 2r_0/\widetilde{d}^2, 0<r_0<\widetilde{d}$ is the probability density function of R_0. The detailed derivation of obtaining (a) can refer to [6].

Then we express Δ_b as (12) in the top of next page. In (12), (a) follows from the probability generating functional of HPPP. When $\widetilde{d}/d\to 0$, $y\in[1,0)$, we can approximately obtain (b). In (c), $\delta=2/\alpha$, ${}_2F_1(a,b;c;z)$ is the gaussian hypergeometric function [7].

Substituting $b=1,2$ in (12), we can respectively express Δ_1 and Δ_2 as (13), and then further obtain $M_1(\theta)$ and $M_2(\theta)$.

$$\begin{aligned} \Delta_1 &= exp\left(-\frac{\pi\lambda_b'\delta\theta r_i^{\alpha}\widetilde{d}^{2-\alpha}}{1-\delta}{}_2F_1\left(1,1-\delta;2-\delta;-\theta r_i^{\alpha}\widetilde{d}^{-\alpha}\right)\right) \\ \Delta_2 &= exp\left(\frac{\pi\lambda_b'\delta\theta^2 r_i^{2\alpha}\widetilde{d}^{2-2\alpha}}{2-\delta}{}_2F_1\left(2,2-\delta;3-\delta;-\theta r_i^{\alpha}\widetilde{d}^{-\alpha}\right)\right. \\ &\quad \left.-\frac{2\pi\lambda_b'\delta\theta r_i^{\alpha}\widetilde{d}^{2-\alpha}}{1-\delta}{}_2F_1\left(1,1-\delta;2-\delta;-\theta r_i^{\alpha}\widetilde{d}^{-\alpha}\right)\right) \end{aligned} \tag{13}$$

V. Model Verification

This section validates the accuracy of our theoretical model via extensive Monte-Carlo simulations. The simulation results are obtained by taking average over 1000 runs. Unless otherwise stated, the default parameters in each simulation are set as λ_w = 0.005 WiFi nodes/m^2, λ_t = 1.0/π tags/m^2, d = 50 m, $\widetilde{d}$ = 1 m, P_0 = 1 dBm, σ^2 = -100 dBm, x = 0.5, and α = 3. In all figures, the labels 'Ana.' and 'Sim.' denote the theoretical and simulation results, respectively.

A. Verification of $M_1(\theta)$ and $M_2(\theta)-M_1^2(\theta)$

Fig. 2 shows the impacts of different path-loss exponent α, on the mean of CSP $\mathbb{E}[\mathbb{P}_b^s(\theta)]=M_1(\theta)$ and the variance of

$$
\begin{aligned}
\Delta_b &\overset{(a)}{=} exp\left(-2\pi\lambda_b' \int_{\widetilde{d}}^{d} \left(1-\left(1-\frac{\theta r_0^{\alpha} r_i^{-\alpha}}{1+\theta r_0^{\alpha} r_i^{-\alpha}}\right)^{b}\right) r_i dr_i\right) \\
&= exp\left(-2\pi\lambda_b' \left(\sum_{n=1}^{b}\binom{b}{n}(-1)^{n+1}\theta^n \int_1^{\left(\widetilde{d}/d\right)^{\alpha}} \frac{r_i^{\alpha n}\widetilde{d}^{1-\alpha n} y^{n-\frac{1}{\alpha}}}{\left(1+\theta r_i^{\alpha}\widetilde{d}^{-\alpha} y\right)^n} \widetilde{d}\left(-\frac{1}{\alpha}\right) y^{-\frac{1}{\alpha}-1} dy\right)\right) \\
&\overset{(b)}{\approx} exp\left(-\pi\lambda_b' \left(\sum_{n=1}^{b}\binom{b}{n}(-1)^{n+1}\theta^n \int_1^{0} \frac{r_i^{\alpha n}\widetilde{d}^{2-\alpha n}}{\left(1+\theta r_i^{\alpha}\widetilde{d}^{-\alpha} y\right)^n} \left(-\frac{2}{\alpha}\right) y^{n-\frac{2}{\alpha}-1} dy\right)\right) \\
&\overset{(c)}{=} exp\left(-\pi\lambda_b' \left(\sum_{n=1}^{b}\binom{b}{n}(-1)^{n+1} \frac{\delta\theta^n r_i^{\alpha n}\widetilde{d}^{2-\alpha n}}{n-\delta} {}_2F_1\left(n, n-\delta; n-\delta+1; -\theta r_i^{\alpha}\widetilde{d}^{-\alpha}\right)\right)\right)
\end{aligned}
\tag{12}
$$

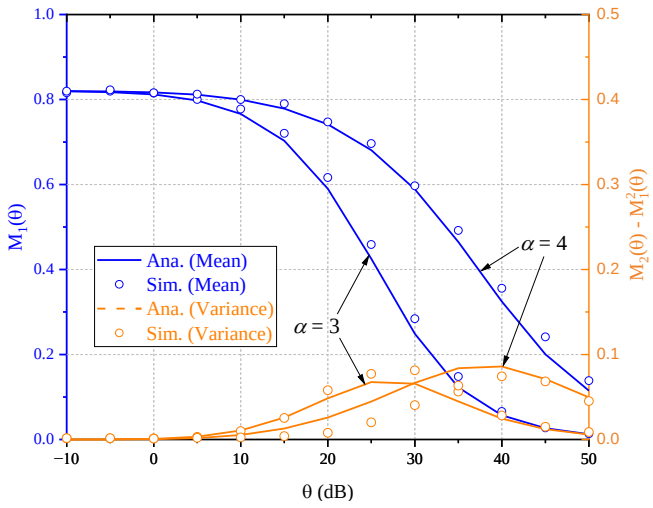

Fig. 2. $M_1(\theta)$ and $M_2(\theta) - M_1^2(\theta)$ vs. θ.

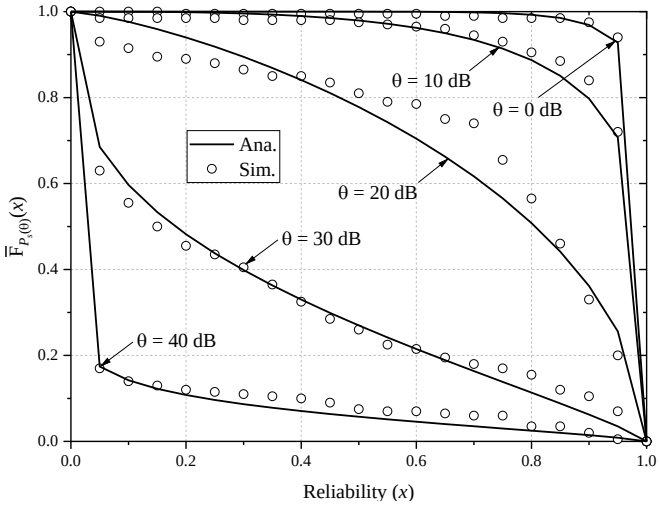

Fig. 3. $\bar{F}_{\mathbb{P}_b^s(\theta)}(x)$ vs. reliability x.

CSP Var$(\theta) = M_2(\theta) - M_1^2(\theta)$ as θ varies from -10 dB to 50 dB. From this figure, we can conclude:

- Given α, $M_1(\theta)$ decreases as θ increases; in contrast, $M_2(\theta) - M_1^2(\theta)$ first increases and then decreases as θ increases.
- Given θ, the larger α, the larger $M_1(\theta)$. The reason is that when α is large, the power of interfering tag signals at the node is small, which leads to a high SINR and a high successful transmission probability. Hence, $M_1(\theta)$ is large.
- Given θ, when θ is smaller than 30 dB, the larger α, the smaller $M_2(\theta) - M_1^2(\theta)$; when θ is larger than 30 dB, the larger α, the larger $M_2(\theta) - M_1^2(\theta)$.

B. Verification of $\bar{F}_{\mathbb{P}_b^s(\theta)}(x)$

Fig. 3 shows the impacts of different SINR threshold θ, on $\bar{F}_{\mathbb{P}_b^s(\theta)}(x)$ as reliability x varies from 0 to 1. From this figure, we can conclude:

- Given θ, $\bar{F}_{\mathbb{P}_b^s(\theta)}(x)$ gradually decreases as x increases. For a smaller θ (i.e., θ = 0 dB), $\bar{F}_{\mathbb{P}_b^s(\theta)}(x)$ first decreases slightly and then decreases rapidly, which means a higher reliability. For a larger θ (i.e., θ = 40 dB), $\bar{F}_{\mathbb{P}_b^s(\theta)}(x)$ first decreases rapidly and then decreases slowly, which means a lower reliability.
- Given x, the larger θ, the smaller $\bar{F}_{\mathbb{P}_b^s(\theta)}(x)$. Particularly, when $x = 0$, $\bar{F}_{\mathbb{P}_b^s(\theta)}(x) = 1$; when $x = 1$, $\bar{F}_{\mathbb{P}_b^s(\theta)}(x) = 0$.

VI. Conclusion

This paper presents an MD-based fine-grained analysis to characterize the disparity among individual backscatter transmission links in CWBNs. Using stochastic geometry, this study derives the mathematical expressions for the b-th moments of conditional success probability and MD. The extensive Monte-Carlo simulations have been conducted and the results well confirm the accuracy of the proposed theoretical model, thus allowing engineers to well understand the overall performance of CWBNs. Our future work aims to adopt more suitable spatial distributions to model the location of nodes and tags and explore more performance metrics.

REFERENCES

[1] Z. Wang, L. Feng, S. Yao, K. Xie, and Y. Chen, "Low-cost and long-range node-assisted WiFi backscatter communication for 5G-enabled IoT networks," *Wireless Communications and Mobile Computing*, vol. 2021, 2021.

[2] Z. Ma, L. Feng, and F. Xu, "Design and analysis of a distributed and demand-based backscatter MAC protocol for Internet of Things networks," *IEEE Internet of Things Journal*, vol. 6, no. 1, pp. 1246–1256, 2018.

[3] X. Cao, Z. Song, B. Yang, M. A. ElMossallamy, L. Qian, and Z. Han, "A distributed ambient backscatter MAC protocol for Internet-of-Things networks," *IEEE Internet of Things Journal*, vol. 7, no. 2, pp. 1488–1501, 2019.

[4] L. Shi, R. Q. Hu, Y. Ye, and H. Zhang, "Modeling and performance analysis for ambient backscattering underlaying cellular networks," *IEEE Transactions on Vehicular Technology*, vol. 69, no. 6, pp. 6563–6577, 2020.

[5] Q. Wang, Y. Zhou, H.-N. Dai, G. Zhang, and W. Zhang, "Performance on cluster backscatter communication networks with coupled interferences," *IEEE Internet of Things Journal*, vol. 9, no. 20, pp. 20 282–20 294, 2022.

[6] Y. Wang, Q. Zhao, S. Yao, L. Feng, and H. Liang, "Performance modeling of tags-to-WiFi transmissions for contention-based WiFi backscatter networks," in *2022 IEEE International Conference on Networking, Sensing and Control (ICNSC)*. IEEE, 2022, pp. 1–6.

[7] M. Haenggi, "The meta distribution of the SIR in Poisson bipolar and cellular networks," *IEEE Transactions on Wireless Communications*, vol. 15, no. 4, pp. 2577–2589, 2015.

[8] M. Haenggi, "Meta distributions—part 1: Definition and examples," *IEEE Communications Letters*, vol. 25, no. 7, pp. 2089–2093, 2021.

[9] M. Haenggi, "Meta distributions—part 2: Properties and interpretations," *IEEE Communications Letters*, vol. 25, no. 7, pp. 2094–2098, 2021.

[10] N. Deng and M. Haenggi, "A fine-grained analysis of millimeter-wave device-to-device networks," *IEEE Transactions on Communications*, vol. 65, no. 11, pp. 4940–4954, 2017.

[11] M. Shi, X. Gao, K. Yang, D. Niyato, and Z. Han, "Meta distribution of the SINR for mmwave cellular networks with clusters," *IEEE Transactions on Communications*, vol. 69, no. 10, pp. 6956–6970, 2021.

[12] Y. Qin, M. A. Kishk, and M.-S. Alouini, "A dominant interferer plus mean field-based approximation for SINR meta distribution in wireless networks," *IEEE Transactions on Communications*, 2023.

[13] M. Shi, K. Yang, D. Niyato, H. Yuan, H. Zhou, and Z. Xu, "The meta distribution of SINR in UAV-assisted cellular networks," *IEEE Transactions on Communications*, vol. 71, no. 2, pp. 1193–1206, 2022.

[14] Y. Qin, M. A. Kishk, and M.-S. Alouini, "On the downlink SINR meta distribution of UAV-assisted wireless networks," *IEEE Transactions on Communications*, 2023.

[15] D. Bharadia, K. R. Joshi, M. Kotaru, and S. Katti, "Backfi: High throughput WiFi backscatter," *ACM SIGCOMM Computer Communication Review*, vol. 45, no. 4, pp. 283–296, 2015.

[16] Q. Wang, Y. Zhou, H.-N. Dai, G. Zhang, M. Imran, and N. Nasser, "Modeling and analysis of finite-scale clustered backscatter communication networks," in *ICC 2023-IEEE International Conference on Communications*. IEEE, 2023, pp. 1456–1461.

[17] Z. Fang, Q. Li, J. Liu, J. Zhou, and S. Shen, "Beamforming design for multi-antenna multi-tag symbiotic radio backscatter systems," *AEU-International Journal of Electronics and Communications*, vol. 170, p. 154820, 2023.

[18] Y. Liu, H.-N. Dai, M. Imran, and N. Nasser, "Ground-to-UAV communication network: Stochastic geometry-based performance analysis," in *ICC 2021-IEEE International Conference on Communications*. IEEE, 2021, pp. 1–6.

[19] Y. Wang, L. Feng, S. Yao, H. Liang, H. Shi, and Y. Chen, "Outage probability analysis for D2D-enabled heterogeneous cellular networks with exclusion zone: A stochastic geometry approach," *CMES-Computer Modeling in Engineering & Sciences*, vol. 138, no. 1, pp. 639–661, 2024.

[20] Y. Liu, H.-N. Dai, and N. Zhang, "Connectivity analysis of UAV-to-satellite communications in non-terrestrial networks," in *2021 IEEE Global Communications Conference (GLOBECOM)*. IEEE, 2021, pp. 1–6.